Available online at www.sciencedirect.com
SCIENCE DIRECT
Powder Technology 165 (2006) 1 – 10
POWDER TECHNOLOGY
www.elsevier.com/locate/powtec

Image analysis of particles by modified Ferret method — best-fit rectangle

Weixing Wang *

School of Electronic Engineering, University of Electronic Science and Technology of China, Post code: 610054, China

Received 17 January 2005; received in revised form 18 August 2005; accepted 22 March 2006
Available online 24 May 2006

Abstract

For the purpose of choosing and designing measurement algorithms to characterize particle size and shape rotation-invariantly, reproducibly, simply, and reasonably, this paper presents an image analysis measurement algorithm-best-fit rectangle for particle size and shape. The best-fit rectangle approach is a combination of the Ferret method and the least 2nd moments minimization, only requiring calculation of three moments about the center of gravity, and maximum and minimum co-ordinates in a co-ordinate system oriented in the direction of the axis of the least 2nd moments, and a simple area ratio. It is a simple rotation-invariance method, reflecting shape (elongation and angularity). In this paper, the method that has been tested in a large number of aggregate particle samples in a laboratory is introduced theoretically in detail, analyzed and compared to other widely used methods. The test results show that by using this method, the results are very close to manual measurements (for size, elongation and angularity). The width accumulative curve is parallel to the curves of sieving and thickness, implying that sieving analysis and thickness measurement can be easily estimated by the width. The method combining other image processing algorithms in an online system does the processing in real time. It is more reasonable and useful than other traditionally used measurement methods in image analysis.

Keywords: Image analysis; Particle size and shape; Ferret method; Least 2nd moments; Elongation; Angularity

1. Introduction

The determination and measurement of the size and shape of particles are carried out in many engineering fields. There are certain relationships between the shape and the size when particles are measured. In the fields of geology, metallurgy, agriculture, concrete and aggregates engineering, the variation of size and shape of particles is large, therefore, the size and shape determination is quite complex.

Image analysis techniques have been used for particle size measurement in the last twenty years [1–19]. As computers are widely used today, the cost of an image system is low, and particle size and shape analysis can be handled easily and fast. Within image analysis two-dimensional images are normally analyzed. The image analysis techniques rely on first obtaining a digitized outline of each individual particle from a photograph or a video film, then measuring the size and shape parameters of the particle by computer and software. In image analysis, different ways of measuring particle size, such as chord size [1–4], equivalent circle diameter [5–10], maximum size [11–13], size of equivalent ellipse [14,15], and simple Ferret diameter [16–19] have been used. A reasonable representation of particle size should reflect the shape of particles. It can also be application dependent. Size determination used in the previous studies [1–19], was often based on traditional measuring methods, not image analysis. Few researchers analyze if the determinations are reasonable in discrete image measuring procedures.

In what follows, we describe and analyze the suggested particle size measurement method — the best-fit rectangle algorithm, together with testing results using image analysis. In Section 2, we explain the reason why we choose the best-fit rectangle algorithm to measure aggregate particle size and shape. Section 3 introduces the algorithm, combining the Ferret method and the method for obtaining the orientation of a particle (least 2nd moments), and

* Present address: Department of Computer Science and Technology, Chongqing University of Posts and Telecommunications, 400065, China.
E-mail addresses: wangwx@cqupt.edu.cn, znn525d@yahoo.com.

0032-5910/$ - see front matter © 2006 Elsevier B.V. All rights reserved.
doi:10.1016/j.powtec.2006.03.017

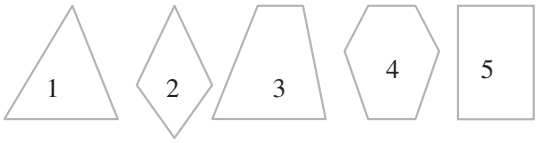

Fig. 1. Classification of crushed aggregate particles.

describes the measurement parameters based on the best-fit rectangle. Section 4 gives examples in experiments, and a comparison is made between the algorithm measurement and laboratory measurement of actual aggregate particles. Finally, Section 5 discusses and analyzes the algorithm by comparing with other methods.

2. Basic considerations for a method of aggregate particle size and shape measurement

Based on investigations, any method for aggregate size and shape measurements should meet the following requirements:

(1) A method should have a size definition in which no matter how a particle is positioned in an image, the measured size should be unique, independent of image scanning direction or particle rotation, which is called rotational-invariance.
(2) The first shape parameter is Elongation. Flakiness (the ratio between thickness and length) or Elongation (the ratio between width and length) is a very important piece of information in an aggregate industry in addition to particle size. Mora and Kwan, in their study [18], described several shape factors as functions of Elongation.
(3) The second shape parameter is angularity and should be robust. In Ref. [18], the authors found that the definition of angularity varies among different researchers, and the traditional method or definition is un-reasonable. Here, we mean crude expression of angularity, not angularity description in detail. Two particles may have the same size and elongation, but different angularities. This parameter is also an important information in aggregate industry.
(4) The measurement itself should be as simple as possible. Complicated algorithms or measurements are not necessarily suitable for multiple aggregate particle measurements (e.g. for an online system). As it is well known, Fourier and Fractal measurement methods are very good for characterizing particle size and shape, they are suitable for a single particle, but not for statistical analysis of multiple aggregate particles.

Table 1
Evaluation of the existing particle size and shape measurement methods

Methods	Rotational-invariance	Elongation	Angularity	Simple
Chord sizing	No	No	No	Yes
Simple Ferret	No	No	No	Yes
Maximum diameter	Yes	No	No	No
Equivalent circle	Yes	No	No	Yes
Equivalent ellipse	Yes	Yes, not 100%	No	No
Multiple Ferret	Yes, but not 100%	Yes	Yes, not 100%	No

If a method of aggregate particle size measurement by image analysis meets the above four basic conditions, the measurement will be stable and fast, and size and shape can be reproducible. Based on the four conditions, let us classify aggregate particles, analyze and evaluate the existing and widely used methods [20].

2.1. A model of aggregate particles

As investigated, if one uses a bounded rectangle to characterize the shape of a particle, the area ratio (R) between a particle and its bounded rectangle may be a parameter to show the shape or rectangularity (angularity). It is convenient to classify the crushed aggregate particles into five basic shapes (see Fig. 1):

a) triangle-like: a particle with three main sides, R will be about 50%;
b) diamond-like: a particle with four main sides, but R will be about 50–60%;

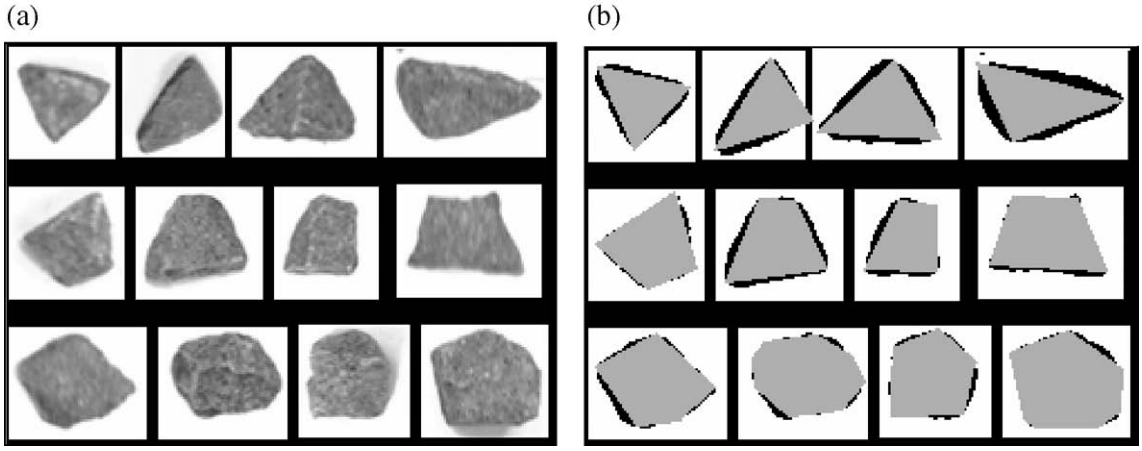

Fig. 2. Shapes of crushed aggregate particles. (a) The original image includes 12 particles. (b) Particles are constructed by triangles, diamonds, trapezoids and polygons.

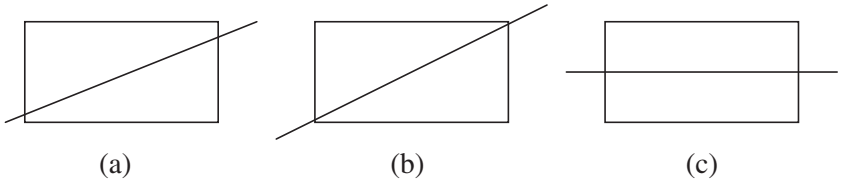

Fig. 3. Three measurements of the orientation of a rectangle object. (a) Multiple Ferret measurement; (b) Maximum length measurement; and (c) Least moment measurement.

c) trapezoid-like: a particle with four main sides, R will be about 60–90%;
d) polygon-like: a particle with more than four main sides, R will be about 60–90%;
e) rectangle-like: a particle with four main sides, but R will be over 90%.

The corners of categories (2)–(4) particles are somewhat rounded. Note also that we use the suffix "like" to stress that this is a crude shape description of the particle boundary. Fig. 2, shows real particle shapes, where twelve aggregate particles of size 32–64 mm were randomly sampled from a rockpile in a quarry. They represent the five different shapes more or less. This is an underlying model in the discussion and evaluation of methods in this paper. The question is how to make the bounded rectangle — best-fit rectangle for each of the particles by image analysis, and to ensure the size and shape measurement rotation-invariant.

2.2. Comparisons of existing measurement methods

To design a method for aggregate particle size measurement, we should consider the following aspects: (1) aggregate particles locate and orient randomly in an image, so we cannot expect that orientations of particles are in a certain orientation in an image; (2) aggregate particles are irregular in shape; (3) in a quarry or mining industry, the boundaries of aggregate particles are very rough, owing to either their physical properties or the technique of the photograph or image digitizing; and (4) aggregate particles even having the same size or elongation may have extremely different shapes.

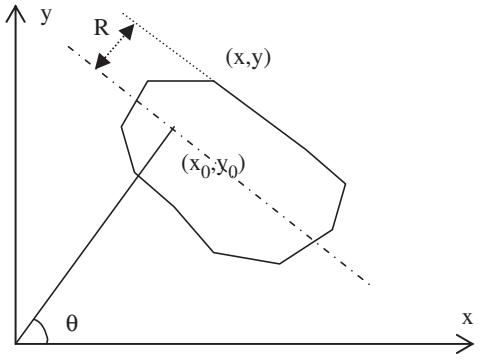

Fig. 4. Least-second moment measurement for obtaining the orientation of a particle: The perpendicular distance from a point (x, y) to a line which pass through the center of an object.

Table 1 shows a comparison of six measurement methods. One can see that the Multiple Ferret method meets best the four conditions described above. The remaining question is to improve it, which is the topic of the next section.

3. The method of best-fit rectangle

Empirically, as mentioned, the shapes of crushed aggregates vary between triangular-like, diamond-like, trapezoidal-like, polygon-like and rectangular-like with intermediate shapes in between. To make a measurement method rotationally-invariant, reproducible, of low boundary roughness sensitivity and reflecting crude shape, a new measurement method, called the best-fit rectangle, has been developed. A summary of the measurement sequence is as follows:

(a) Obtain orientation of a particle by using the least-second moment method (= rotationally-invariant) which yields a simple closed formula for the orientation.
(b) Length and width can be obtained by using a Ferret box in the orientation of the least 2nd moments. Thus, rotation-invariant elongation is defined implicitly.
(c) The area ratio in the orientation of the axis of the least 2nd moments yields approximate rectangularity. For crushed or blasted aggregate particles, the manufacturers want to know not only the elongation of a particle, but also angularity or rectangularity, so the area ratio obtained from the Ferret box in the direction of the least 2nd moments is of great practical

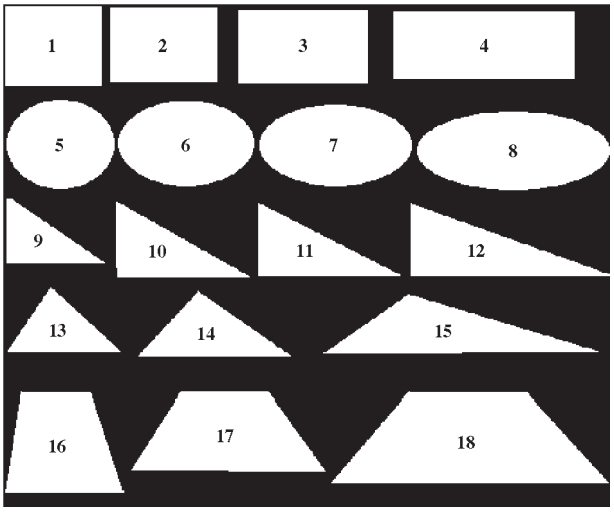

Fig. 5. Particles with different typical shapes.

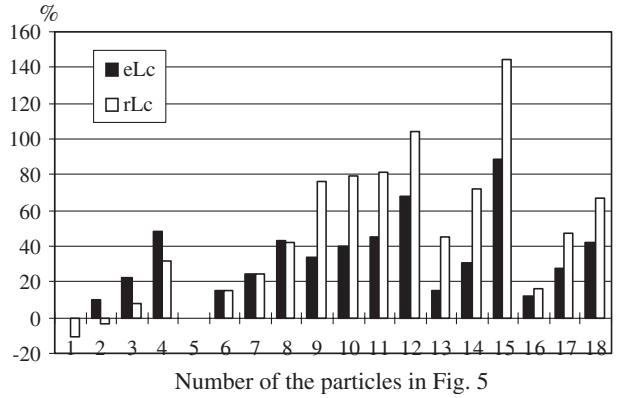

Fig. 6. Comparison of eL, rL and cL.

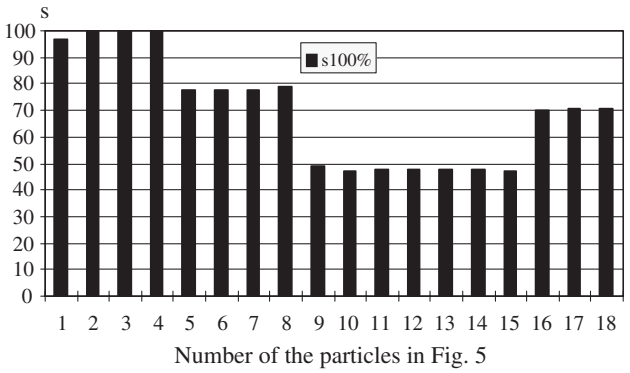

Fig. 8. Particle's angularity in Fig. 5.

importance. It is less practical to find the rectangularity by a discrete minimization procedure over possible Ferret boxes, since many directions need to be investigated in order to safeguard an exact minimum.

The method is mainly a combination of orientation determination algorithm and the Ferret measurement algorithm; therefore, we will give a description for the two algorithms as follows.

3.1. Dot product method (Multiple Ferret)

Before the advent of automatic image analyzers, several quickly measurable parameters were defined, which would help particle size analysts to classify irregular-shaped particles by using a single linear measurement. One of the easiest to measure is the caliper diameter, the distance between two parallel tangents which are on opposite sides of the particle. This method was proposed by L.R. Ferret (1931) [20], and the measurement is often referred to by his name. In systems employing boundary-coding techniques, a single pass around the boundary of an object noting maximum and minimum x and y co-ordinates will yield vertical and horizontal Ferret diameters. This way, the Ferret diameter strongly depends on the direction of system scanning, which is not rotationally-invariant.

By co-ordinate transformation, it is possible to measure the Ferret diameter at any angle to the horizontal. The detailed description (so-called dot products, was mentioned by Fischler, 1980) [21,22] can be summarized as

Let x_i, for $i=1, 2,\ldots, N$ be the sampled boundary points. Let u_j for $j=1, 2,\ldots, D$ be the so-called reference vectors. In one pass, traversing the points $i=1, 2,\ldots, N$ in any order, calculate:

$$x_i^T u_1, x_i^T u_2, \ldots, x_i^T u_D, \tag{1}$$

$$\text{Save only MAX} = \max(x_i^T u_j), \textit{and MIN} = \min(x_i^T u_j) \tag{2}$$

For each $j=1, 2,\ldots,D$, as well as those co-ordinates which give rise to the D maxima and D minima. The combined dot product method and convex hull method can be described as:

As before calculate for $i=1, 2, \ldots, N$:

$x_i^T u_1$, $x_i^T u_2,\ldots x_i^T, u_D$. Save only MAX=max($x_i^T u_j$), together with all other values which are in the interval [MAX−T(MAX−MIN), MAX], and MIN=min($x_i^T u_j$) together with values in the interval [MIN+T(MAX−MIN), MIN], $\forall j$, as well as those co-ordinates which give rise to these values. Call this new subset of points S. For all the points in S calculate the exact diameter using the convex hull method.

The multiple Ferret method, in the sense that max$\{L_1, L_2, \ldots L_D\}$ is chosen as the diameter, coincides with the dot product method, if new scanning directions are implemented using dot products with new co-ordinate axes. The only difference is that the directions

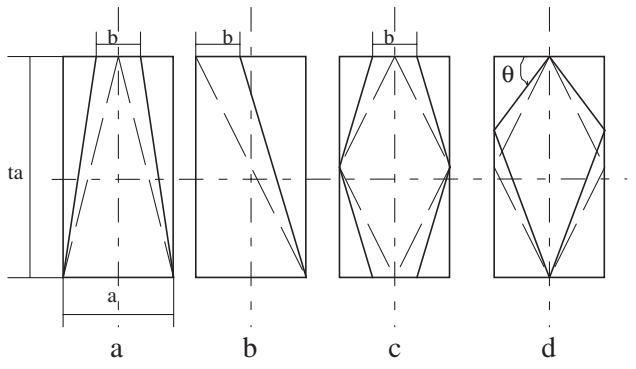

Fig. 7. Four typical shapes of particles.

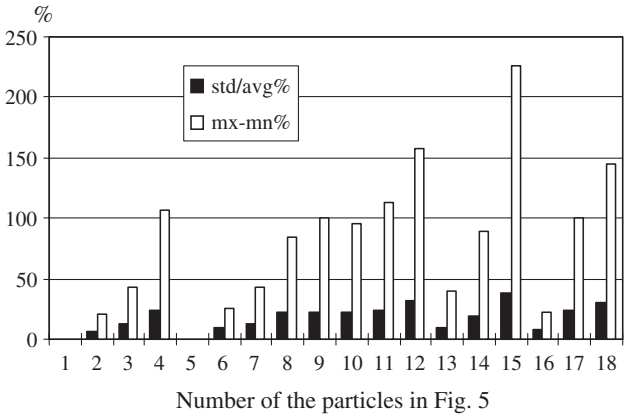

Fig. 9. Elongation with Ferret measurement.

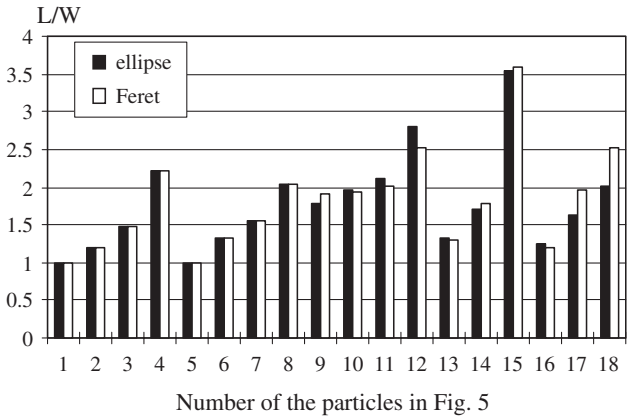

Fig. 10. Elongations of ellipse and Ferret.

chosen are multiples of 2, and multiple Ferret is often not implemented as a one pass algorithm.

In order to resolve the problem of rotation dependence, some image analyzers measure a fixed number of the Ferret diameters, usually 2, 4, 8 or more, and the user may be able to select how many of these are to be measured, then the maximum length can be obtained. In this method, only the length that is approximately close to maximum length can be obtained, the reproducibility and rotationally-invariant cannot be fully achieved. To reduce the calculation and obtain a particle's orientation in one pass, the following orientation algorithm can be used.

3.2. Orientation determination

How precisely do we define the orientation for an object? The usual practice is to choose the axis of length. There are three different measurement methods as shown in Fig. 3:

One way of measuring is to make multiple Ferret measurements (Fig. 3(a)) and select the longest one as approximate length, the axis of length being its orientation, using this method, the orientation depends on how many Ferret measurements are used, which is not rotation-invariant. The second way, the Maximum length measurement (Fig. 3(b)), is to find out the maximum length of the particle. For doing so, one needs to calculate the distances for each pair of boundary pixels. As the bounded rectangle is not a minimal circumscribed rectangle, the two methods described above cannot represent the shape of the particle. The third method, "Least moment measurement" as shown in Fig. 3(c), is the only way to construct the minimal circumscribed rectangle for a particle. Let's review how to find the orientation of a particle by the use of least moment measurement with reference to Fig. 4. Note that least moment measurements aim at determining a suitable orientation of an object, but combining the orientation with the Ferret boxes has not been considered before.

Fig. 4 is a two-dimensional equivalent of the axis of the least inertia. We search for the line for which the integral of the square of the distances between the points in the object and the line is a minimal:

$$E = \iint_I R^2 f(x,y)\,dxdy \tag{3}$$

where R is the perpendicular distance from the point (x, y) to the line sought after; $f(x,y)$ is a binary image.

From Fig. 4, one has:

$$\begin{aligned} E &= \frac{1}{2}\left(I_x + I_y\right) + \frac{1}{2}\left(I_x - I_y\right)\cos 2\theta - \frac{1}{2} I_{xy}\sin 2\theta \\ &= I_x \sin^2\theta - I_{xy}\sin\theta\cos\theta + I_y\cos^2\theta \end{aligned} \tag{4}$$

where $I_x = \iint_{I'}(x')^2 f(x,y)dx'dy'$, $I_y = \iint_{I'}(x'y')f(x,y)dx'dy'$, $I_y = \iint_{I'}(y')^2 f(x,y)dx'dy'$, $x' = x - \bar{x}$ and $y' = y - \bar{y}$; $(\bar{x},\bar{y})$ is the centre of area of the object [23].

Minimization of E gives:

$$\begin{aligned} \sin 2\theta &= \pm \frac{I_{xy}}{\sqrt{I_{xy}^2 + \left(I_x - I_y\right)^2}} \text{ and } \cos 2\theta \\ &= \pm \frac{I_x - I_y}{\sqrt{I_{xy}^2 + \left(I_x - I_y\right)^2}} \end{aligned} \tag{5}$$

Of the two solutions, the ones with the plus signs give the minimum for E, whereas the ones with minus signs correspond to the maximum.

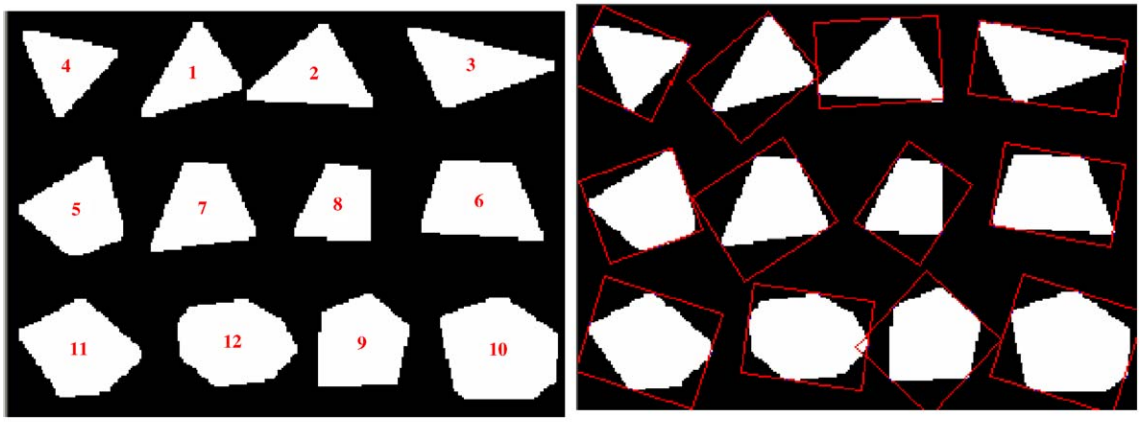

Fig. 11. Segmented real aggregate particles in Fig. 2. (a) The number of each particle has been marked; (b) The best-fit rectangle has been marked for each particle.

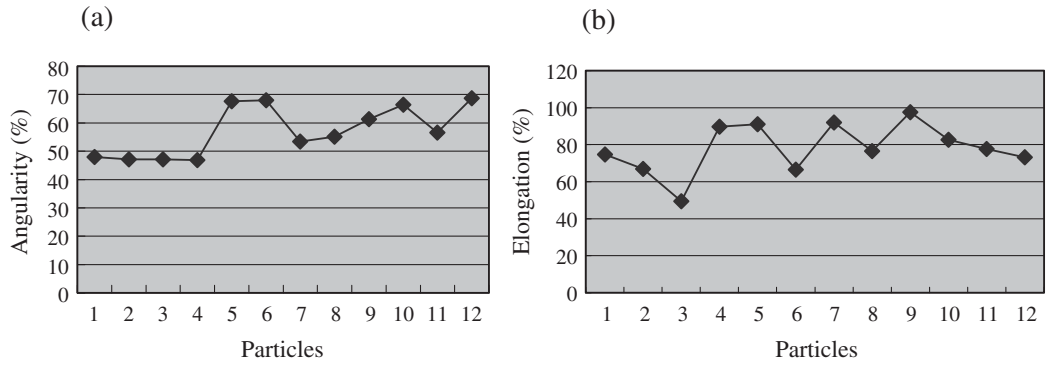

Fig. 12. Shape parameters for particles: (a) angularity (rectangularity); (b) elongation.

For a discrete binary image, we have

$$\tan^2\theta + \frac{I(2,0)-I(0,2)}{I(1,1)}\tan\theta - 1 = 0 \quad (6)$$

where

$$I(p,q) = \sum i^p j^q b(i,j), p,q = 0,1,2 \quad (7)$$

with $b(i, j)$ the binary image, i and j are co-ordinates.

In conclusion, the best way to obtain the orientation of an object is by using least-second moment method, which is rotation-invariant, and the circumscribed rectangle tends to be of minimal area.

3.3. Particle measurement and analysis by best-fit rectangle method

In order to evaluate the method, we designed and created several sets of pictures, each of them including particles of different shapes. Fig. 5 shows one of them, in which, 18 particles with different shapes are created and classified into five groups: (1) No. 1–4 are rectangles; (2) No. 5–8 are ellipses (similar to polygons); (3) No. 9–12 are orthogonal triangles; (4) No. 13–15 are of any kinds of triangles and (5) No. 16–18 are trapezoids. Within every group, the elongation increases from left to right. The image size is 512×512 pixels. The unit of particle size will be in pixels in the following different measurements. In this image, the smallest particle size is more than 80 pixels.

3.4. Size measurement

In order to understand why the curve of best-fit rectangle tends to be higher than the curve of equivalent ellipse in Fig. 6, let us analyze Fig. 5 which presents eighteen typical particles. Fig. 6 illustrates that the best-fit rectangle is better for representing real particle size of crushed particles. For example, the particle No. 1 is almost a square as shown in Fig. 5. The diameter of the equivalent circle of area should be longer than the square length. In this diagram, it shows a negative figure rather than an equivalent ellipse does.

Notes in Fig. 6: eL: length of equivalent ellipse; rL: Length of best-fit rectangle; cL: diameter of circle of equivalent area; eLc: (eL−cL)/cL; rLc: (rL−cL)/cL.

In order to analyze how the method meets the conditions of rotational-invariance, reproducibility and shape representation, we compared our new method with the existing methods in the three aspects.

3.5. Angularity analysis

The particles inside a rectangle, the general shape can be divided into two types. One is trapezoid with a short side on the bottom or top (Fig. 7(a–b)), another is that the long width is on the middle of rectangle (Fig. 7(c–d)). Their rectangularity (angularity: s=100*particle area/bounded rectangle area) changes from 0.5 to 1.0 as the ratio t=b/a changes from 0 to 1.

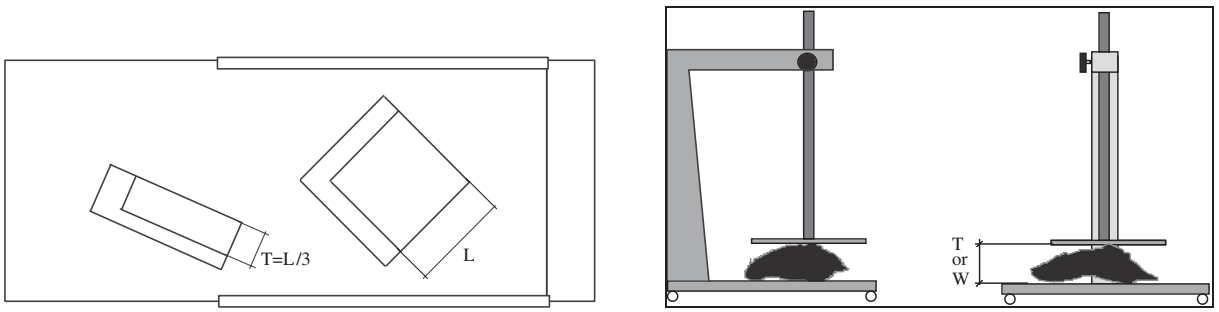

Fig. 13. Aggregate measurement apparatus: (a) for measuring length and index of flakiness, and (b) for measuring width and thickness.

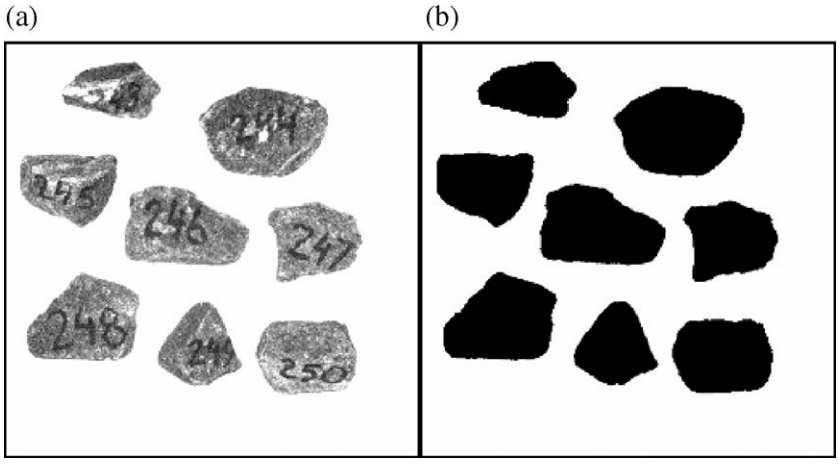

Fig. 14. Images taken under different illuminations. (a) Two bulbs around a camera, gives a diffuse frontlightning illumination. (b) One lighting box gives backlighting illumination.

In Fig. 7, $t=b/a$ $(0\le t\le 1)$, the ratio of the minimum to the maximum widths, when $t=0$, the trapezoids in Fig. 7a–b represent triangles (angularity is 0.5), if $t=1$, they represent rectangles (angularity is 1.0). In Fig. 7(c), when $t=0$, it represents a diamond (angularity is 0.5), if $t=1$, it represents a rectangle (angularity is 0.5). In Fig. 7(d), it always represents a diamond, angularity is 0.5.

From Figs. 5 and 8, we see that particles No. 1–4 are rectangles, and their angularity s values are almost 100. Particles No. 5–8 are ellipses with s values of about 80. Particles No. 9–15 are triangles with s values of about 50. And particles No. 16–18 are trapezoids and their s values are about 70. From the parameter s, the angularities of particles (e.g. crushed and blasted aggregate particles) can be estimated.

3.6. Elongation measurement

Notes: in the Figs. 9 and 10, we use: std/avg% (100 * standard deviation /average value) is defined as the coefficient of variance, and mx − mn% = (maximum value − minimum value)/minimum value × 100, is called max-variance.

In Ferret measurements, particle elongation is not stable; it varies with the direction of scanning. Fig. 9 shows the variance of elongation of the particles in Fig. 5, in nine directions (with angles of 0°, 10°, 20°, 30°, 40°, 50°, 60°, 70°, 80°). As shown in Fig. 10, the ratios (Length/Width) between equivalent ellipse and best-fit rectangles are very close, for almost any kind of shapes. This means that the new method meets the rotation-invariance and reproducibility requirements (refer to Table 1).

In conclusion, the new method provides a better option for particle size measurement than previous methods. By using this method, length, width, elongation and angularity of particles can be measured rotation-invariantly and reproducibly. The algorithm is also easy to implement. After orientation determination according to Eq. (5), the Ferret box can be obtained in the orientation.

3.7. Example of measurements for real particles

In Fig. 11(a), we show 12 segmented real aggregate particles (the number was marked on each of the particles) on Fig. 2.

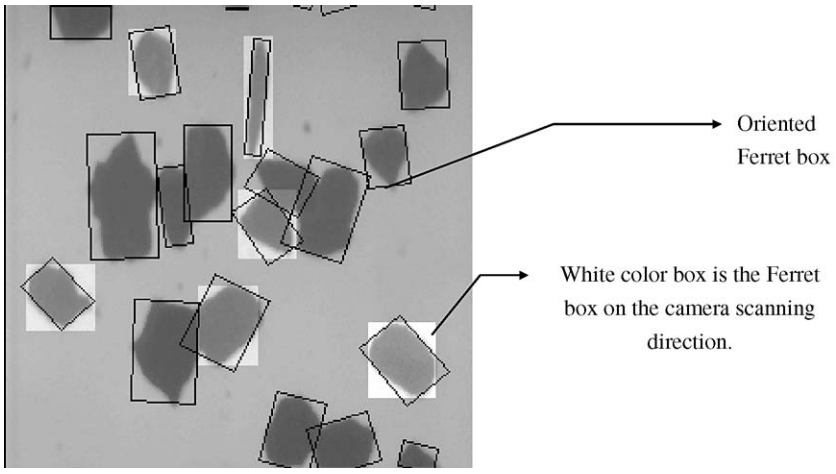

Fig. 15. Size and shape measurement of a particle on an oriented Ferret box.

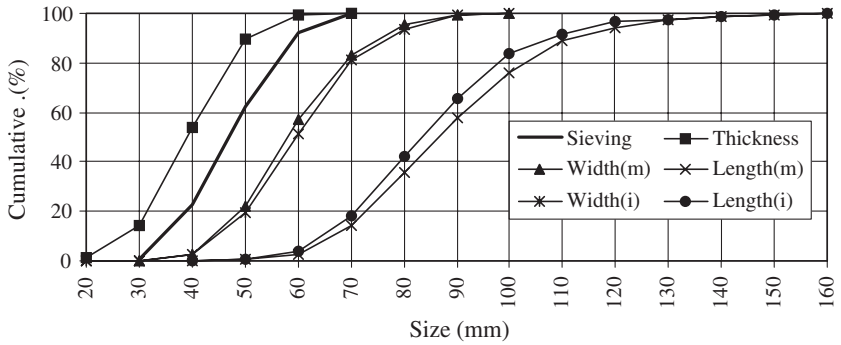

Fig. 16. Size distributions measured by sieving, manual measurements and image analysis.

To avoid small-scale fluctuations along boundaries of aggregate particles, polygonal approximation for every particle (object) is applied. In our case, the goal of a polygonal approximation is to smooth the boundary on a certain scale and obtain the significant boundary segment lines. The boundary can be approximated with varying precision. Here, we just use a maximum of eight segment lines to construct a polygon for each of the particles. The detailed information for the polygonal approximation we used can be found Ref. [24]. The best-fit rectangles constructed by using our new method, are displayed in Fig. 11(b). Particles' elongations and angularities are illustrated in Fig. 12. The particles of triangular shape (No. 1–4 in Fig. 12(a)), have angularities about 50% (or 0.5), but with varying elongations. The particles of trapezoidal or polygonal shape (No. 5–12 in Fig. 12(a)) have a range of angularity between 0.58 to 0.70, and elongations varying from 0.62 to 0.98. This is a reasonable situation: triangles (or diamonds) and rectangles can be easily distinguished from other shapes by using our crude angularity definition, and elongation is independent of angularity. Further detection of particle shapes is needed for more detailed analyses (see Conclusions and further studies).

4. Experimental results

4.1. Measurement by sieving, manual measurements and image analysis

Sieving is one of the oldest methods of aggregate analysis and is accomplished by passing a known weight of sample material successively through finer sieves and weighing the amount collected in each sieve to determine the percentage weight in each size fraction. Test sieves are designed by the nominal aperture size, which is the nominal central separation of opposite sides of a square aperture, rectangle, or the nominal diameter of a round aperture. A variety of sieve aperture ranges are currently used. In our case, we used a square aperture of sieves. A series of sieves with square apertures 27, 32, 38, 45, 54 and 64 mm was used.

In the normal test procedure of sieving analysis, the material to be tested is placed in the uppermost, coarsest sieve, and the nest is then placed in a sieve shaker which vibrates the material in a vertical plane, and, in some models, a horizontal plane. After the required vibration time, the nest is taken apart together with the material retained in each sieve. We could not do our sieving test in this way due to particle size being too big and not having powerful equipment. Instead, every crushed aggregate particle was measured manually by putting it through sieves with different angles, the measured sieve size being marked with the minimum sieve size through which a particle can pass. Meanwhile, the particle was weighted on an electronic weighing apparatus.

Sieving size is just a size as measured by sieves; it cannot provide any other dimensional information. To compensate for this, we manually measured crudely three dimensions of every particle in our laboratory. As a general consideration, the manual measurement might be person-dependent. In order to eliminate subjective measurement errors, two engineers did the measurement together. In this manual measurement, we used two types of apparatus as shown in Fig. 13(a–b). One, as a standard apparatus, is for measuring length and an index of flakiness (the index only indicates if a particle has a flakiness over 1/3); the rectangle size of the apparatus can be adjustable for the length of a particle. The other one was made by us for measuring the thickness (T) and the width (W) of a particle (see Fig. 13(b)).

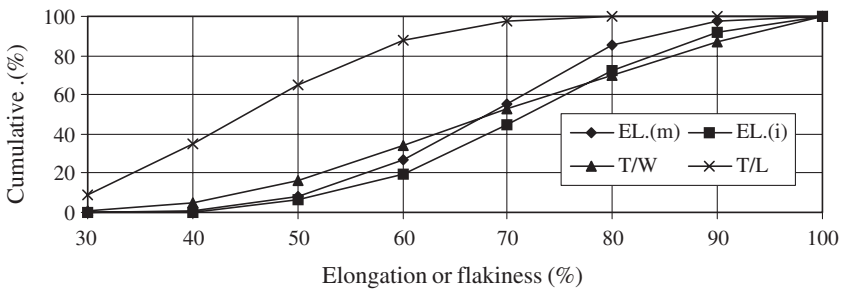

Fig. 17. Comparison between different elongations and flakinesses.

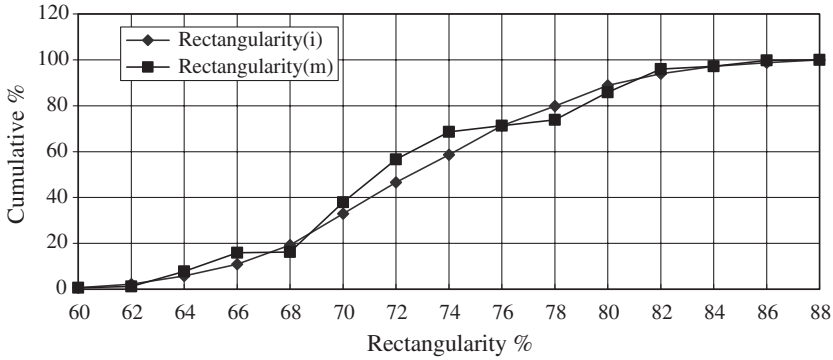

Fig. 18. Comparison of rectangularity distributions. Rectangularity (m) and Rectangularity (i) are obtained from a laboratory test.

For image analysis, aggregate particles were placed on a white plane to contrast with the color of the particles, and separated manually to ensure that every particle was in a stable position. A camera was installed above the plane. Good illumination was controlled by light sources (both frontlightning and backlightning illuminations). The captured images are of a fairly good quality (see Fig. 14). The samples were analyzed by our image systems. Image segmentation programs are interactive programs which can be used by an operator to exactly delineate every particle in an image. The lengths, widths, elongations, rectangularity and areas of particles were measured by using the algorithm-best-fit-rectangle described in the previous section, which is also shown in Fig. 15. The number of aggregate particles for comparison between image analysis and manual measurement was up to 2000.

4.2. Comparison between sieving, manual measurements and image analysis in a laboratory

In the following weighted distribution curves, sieving and manual measurements are weighted by weight, and image measurements are weighted by area*λ (e.g. λ=average width *0.75: experiment constant) [19]. In order to distinguish manual measurements from image analysis, we assign a mark (*m*) for manual measurements and a mark (*i*) for image measurements.

Fig. 16 shows the results. It can be seen that the width of the image analysis compares well with that of manual measurements, but deviates from that of the sieving analysis. The sieving analysis curve is located in between the curves of particle thickness and widths, the curves are parallel to each other, which maybe important information for the estimation of particle thickness and sieving analysis results. The comparison of the lengths shows that the image analysis curve is slightly shifted to the left compared with the curve of the manual measurements. The reason for this may be that it is difficult to obtain the exact lengths of aggregates by manual measurements. For a given width, a small length *L* will give a small elongation, which explains why the curve of elongation (*i*) is to the left of that of elongation (*m*), as shown in Fig. 16. In Fig. 16, the flakiness curve has a much higher cumulative percentage than the other curves do. The comparison of the results also shows that the particles in this sample have the property that *W*/*L* is close to *T*/*W* (Fig. 17).

In manual measurement, the result is that class (1) triangle is 13.68%; (2) diamond 29.1%; (3) trapezoid 13.71%; (4) polygon 22.64%; and (5) rectangle 20.72%. In Fig. 18, it crudely presented the results. If we assume that manually classified triangles and diamonds have rectangularity in the range of 51–71, and rectangles have rectangularity in a range over 80, the two measurements (manual and image) fit well (cf. Fig. 18).

4.3. Online measurement

One system for gravity flow was set up in a quarry in Sweden. A CCD camera grabs aggregate images from the gravity flow. The software firstly detects the image to see if it includes aggregates, and if not, omits that image, which is a procedure we call automatic selection of aggregate images. For a selected image, the optimal

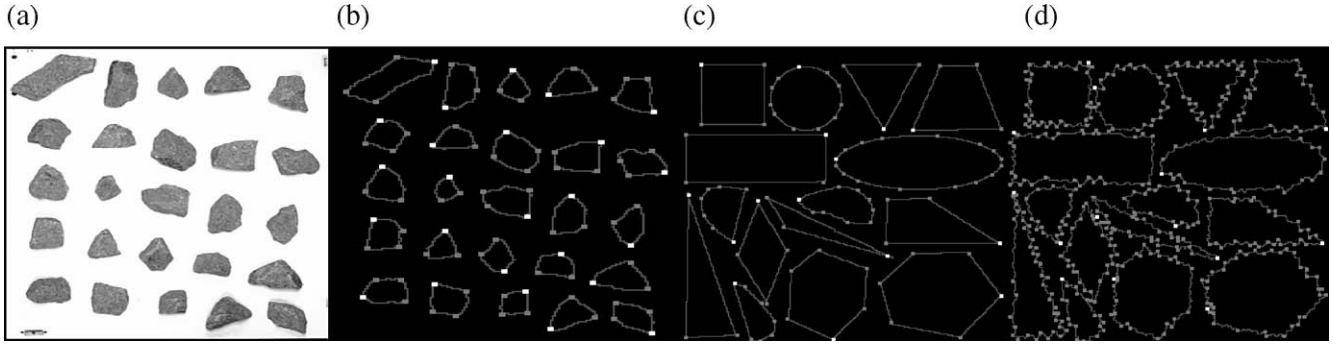

Fig. 19. Polygonal approximation for crushed aggregates: (a) Original image; (b) Resulting image of polygonal approximation; (c) Shape detection (without concave vertices) on a drawing image; (d) Roughness detection (many convex vertices) on a drawing image. Notes: all the nodes represent the detected vertices (corners); the white nodes represent the sharpest corners for every particle.

thresholding algorithm is applied to binarize the aggregate image [25]. Then a splitting algorithm detects the touching aggregates and splits them. Finally, an algorithm involving oriented Ferret boxes is used for analysis of size and shape of aggregates (see Fig. 15, a part of an image). For a normal PC (image size 512 × 512 pixels) in a PC (2 Ghz) in Windows 2000 environment, about 5000 aggregate particles (50–100 images) can be processed in a few seconds (1–2 s). The measurement accuracy is 97%, comparing to manual measurement. The system does the processing in real time.

5. Conclusions and further studies

The best-fit rectangle method works very well for image analysis. It is particularly good for solid particles such as crushed aggregate particles, which can be classified into five basic types of shape: Triangle-like, Diamond-like, Trapezoid-like, Polygon-like and Rectangle-like. The method is rotational-invariant, reflects well the shape (elongation and angularity), and is simple. The test results show that by using this method, the measurement results agree well with manual measurements (for size, elongation and angularity). The accumulative width curve is parallel to the curves of sieving and thickness, implying that sieving analysis and thickness measurement can be easily estimated by the width.

The measurement method of the best-fit rectangle only gives general information about the shapes of particles. In order to obtain more detailed information on particle shape and boundary roughness, corner detection by polygonal approximation might be a possible way. To illustrate this, two simple examples are given in Fig. 19. From the detected corners, the number of corners on the boundary, the angle of each corner, and the segment length between two neighboring corners in each particle can be obtained. Based on this information, natural and crushed particles can be distinguished, and the shapes of triangle, trapezoid, rectangle and polygon for crushed aggregates can be determined too. In Fig. 19, all the spots (or nodes) on boundaries of particles represent the detected corners. The ones with white color show the sharpest corner for each particle. In addition to the shape detection, the algorithm can also detect the boundary roughness of particles as shown in Fig. 19. The particles in Fig. 19(c–d) have similar forms, but the particles in Fig. 19(d) have higher degrees of roughness than those shown in Fig. 19(c). To characterize particles shape and roughness in detail, we will study this subject in the near future.

References

[1] E. Gallagher, Optoelectronic coarse particle size analysis for industrial measurement and control. PhD thesis, University of Queensland, Dept. of Mining and Metallurgical Engineering, 1976.

[2] T. Langer, Real-time measurement of the size distribution of rocks on a conveyor belt, Int. Fed. Automatic control, Workshop on applied Measurements in Mineral and Metal Processing, Johannesburg, October 1988.

[3] T.B. Lang, Measurement of the size distribution of rock on a conveyor belt using machine vision. PhD thesis, the Faculty of Engineering, University of the Witwatersrand, Johannesburg, 1990.

[4] C.L. Lin, J.D. Miller, The development of a PC image-based on-line particle size analyzer, Minerals & Metallurgical Processing 2 (1993) 29–35.

[5] N.H. Maerz, J.A. Franklin, L. Rothenburg, D.L. Coursen, Measurement of Rock Fragmentation by Digital Photoanalysis, 5th. Int. Cong. Int. Soc. Rock Mech., vol. 1, 1987, pp. 687–692.

[6] C. McDermott, G.C. Hunter, N.J. Miles, The application of image analysis to the measurement of blast fragmentation, Proceedings of the Surface Mining—Future Concepts, Nottingham University, Marylebone Press, Manchester, 1989, pp. 103–108.

[7] S.G. Grannes, Determine size distribution of moving pellets by computer image processing, in: R.V. Ramani (Ed.), Proceedings of the 19th Application of Computers and Operations Research in Mineral Industry, Soc. Mining Engineers, Inc., 1986, pp. 545–551.

[8] C. Donald, B.E. Kettunen, On-line size analysis for the measurement of blast fragmentation, in: J.A. Franklin, T. Katsabanis (Eds.), Measurement of Blast Fragmentation, Rotterdam, Balkema, 1996, pp. 175–177.

[9] N.H. Maerz, T.C. Palangio, J.A. Franklin, WipFrag image based granulometry system, in: J.A. Franklin, T. Katsabanis (Eds.), Measurement of Blast Fragmentation, Rotterdam, Balkema, 1996, pp. 91–99.

[10] S.A. Rholl, Photographic assessment of the fragmentation distribution of rock quarry muckpiles, Proceedings of the 4th Int. Symposium Rock Fragmentation by Blasting, Vienna, Austria, 1993, pp. 501–506.

[11] J.J. Montoro, E. Gonzalez, New analytical techniques to evaluate fragmentation based on image analysis by computer methods, Proceedings of the 4th Int. Symposium Rock Fragmentation by Blasting, Vienna, Austria, 1993, pp. 309–316.

[12] A. Ord, Real time image analysis of size and shape distributions of rock fragments, Proc. Aust. Int. Min. Metall, vol. 294, 1, 1989.

[13] J. Kemeny, A practical technique for determining the size distribution of blasted benches, waste dumps, and heap-leach sites, Mining Engineering 46 (11) (1994) 1281–1284.

[14] K.K. Girdner, J.M. Kemeny, A. Srikant, R. McGill, The split system for analyzing the size distribution of fragmented rock, in: J.A. Franklin, T. Katsabanis (Eds.), Measurement of Blast Fragmentation, Rotterdam, Balkema, 1996, pp. 101–108.

[15] J. Schleifer, R. Chavez, N. Cheimanoff, Correlation entrefracturation avant et apres tir par analyze d'images, Proceedings of Abattage des roches al' exlposif, rock blasting, ales, September 1993, pp. 6–10, (France).

[16] G. Blot, J.L. Nissoux, Les nouveaux outils de controle de la granulométrie et de la forme (New tools for controlling size and shape of aggregates), J. Mines etcarriéres, Les Techniques V/94, SUPPL.-Déc., vol. 96(1994), France.

[17] M. Von Hodenberg, Monitoring crusher gap adjustment using an automatic particle size analyzer, Mineral Processing 37 (1996) 432–437.

[18] C.F. Mora, A.K.H. Kwan, Sphericity, shape factor, and convexity measurement of coarse aggregate for concrete using digital image processing, Cement and Concrete Research 30 (2000) 351–358.

[19] C.F. Mora, A.K.H. Kwan, H.C. Chan, Particle size distribution analysis of coarse aggregate using digital image processing, Cement and Concrete Research 28 (6) (1998) 921–932.

[20] W.X. Wang, J. Fernlund, Shape Analysis of Aggregates, KTH-BALLAST Rapport no. 2, KTH, Stockholm, Sweden, 1994.

[21] G. Arfken, Scalar or Dot Product (§1.3.), Mathematical Methods for Physicists, 3rd ed, Academic Press, Orlando, FL, 1985, pp. 13–18.

[22] H. Jeffreys, B.S. Jeffreys, Scalar Product (§2.06.), Methods of Mathematical Physics, 3rd ed., Cambridge University Press, Cambridge England, 1988, pp. 65–67.

[23] B.K.P. Horn, Robot Vision, Londen, England, 1986, pp. 49–62.

[24] W.X. Wang, Binary image segmentation of aggregates based on polygonal approximation and classification of concavities, Pattern Recognition 31 (10) (1998) 1503–1524.

[25] W.X. Wang, Image analysis of aggregates, Computers and Geosciences 25 (1999) 71–81.